Original Article

FABP5 reprograms lipid metabolism and promotes cutaneous T-cell lymphoma progression via activation of PPARγ signalling

Shiwen Wang[1], Sha Jin[1], Shiyu Jin[1], Chenyu Tang[1], Mengyan Zhu[1], Yige Zhao[1], Yangyang Ma[1], Jiaqi Wang[1], Ping Wang[1]

[1]Department of Dermatology, Hangzhou Third People's Hospital, Hangzhou Third Hospital Affiliated to Zhejiang Chinese Medical University, Hangzhou, China

Abstract

Background: Cutaneous T-cell lymphoma (CTCL) constitutes a rare and heterogeneous group of T-cell lymphomas with an unclear pathogenesis. There is emerging evidence that fatty acid binding protein 5 (FABP5) regulates the PPARγ signalling pathway through its binding to fatty acids. However, the precise biological role of FABP5 in CTCL remains unclear.

Aim: To investigate the expression of FABP5 in CTCL and evaluate the effects of targeting FABP5 on the biological behaviors of CTCL tumour cells.

Methods: We performed single-cell transcriptomic analysis to evaluate the expression of FABP5, fatty acid synthase (FASN), and cholesterol regulatory element binding protein (SREBP1) in CTCL patients. FABP5 was knocked down using short interfering RNA (siRNA) lentiviruses, and mRNA expression of FABP5 in CTCL cell lines was quantified by real-time quantitative reverse transcription PCR (RT-qPCR). Cell proliferation and invasion were assessed using CCK-8 and transwell assays, while apoptosis and cell cycle distribution were analysed by flow cytometry. The impact of FABP5 on epithelial-mesenchymal transition (EMT) was investigated via qRT-PCR and Western blot. Intracellular levels of free fatty acids (FFAs), total cholesterol (TC), and triglycerides (TG) were measured with assay kits. The effect of BMS-309403 (a competitive inhibitor of FABP5) on the biological behavior of CTCL cells was also studied.

Results: FABP5 expression was significantly elevated in CTCL patients and cells compared to healthy controls, and silencing FABP5 inhibited cell proliferation. FABP5 knockout upregulated E-cadherin and downregulated N-cadherin and vascular endothelial growth factor (VEGF), thereby inhibiting EMT. Intracellular levels of FFAs, TC, and TG were also reduced. Bristol-Myers Squibb-309403 (BMS-309403) decreased cell viability, induced apoptosis, and lowered TC, TG, and peroxisome proliferator-activated receptor-γ (PPARγ) levels.

Limitations: The study relied solely on in vitro experiments using cell lines. Animal models would strengthen the translational relevance of the findings. In addition, the precise molecular interactions between FABP5 and PPARγ signalling in CTCL remain unclear.

Conclusion: Our findings suggest that the FABP5/PPARγ axis is a promising therapeutic target in CTCL, with BMS-309403 emerging as a potential agent to reverse lipid metabolic reprogramming in CTCL.

Key words: Cutaneous T cell lymphoma, FABP5, lipid metabolism, mycosis fungoides, skin tumour

Corresponding author: Dr. Ping Wang, Department of Dermatology, Hangzhou Third People's Hospital, Hangzhou Third Hospital Affiliated to Zhejiang Chinese Medical University, Hangzhou, China. dermwang@aliyun.com

Introduction

Primary cutaneous T-cell lymphoma (CTCL) is a rare form of non-Hodgkin's lymphoma, accounting for 75% to 80% of all primary cutaneous lymphomas. The most common clinical subtype is mycosis fungoides (MF).[1] In its early stages, CTCL follows a distinct disease progression pattern with relatively indolent biological behavior, but in advanced stages, it can lead to significant morbidity and mortality. Understanding the pathogenesis and focusing on early intervention during the malignant evolution of CTCL are crucial for improving survival quality and prognosis.

Metabolic reprogramming is a well-established hallmark of cancer and has been explored as a potential anti-cancer strategy.[2] The reprogramming of lipid metabolism has recently emerged as a novel feature of cancer, focussing attention on the role of fatty acid (FA) metabolism in oncogenesis.[3,4] Evidence is emerging that FAs are crucial energy sources supporting the proliferation, survival, and tumourigenesis of cancer cells.[5] They bind to fatty acid-binding proteins (FABPs) to facilitate transport,[6] and one member of the family - FABP5 (also known as epidermal FABP), is expressed in various tissues to regulate FA binding, trafficking, and cell growth.[7]

Recent studies have shown that FABP5 is upregulated in several cancer types, including liver, colorectal, ovarian, breast, and prostate cancers, and is often associated with poor prognosis.[8] Higher FABP5 expression has been observed in CTCL lesions.[9,10] Fatty acid synthase (FASN), a key enzyme in FA biosynthesis, is also highly expressed in CTCL cells, and inhibiting both FASN and the cholesterol-regulatory element-binding protein (SREBP) impairs cell survival and proliferation.[11] Our prior analysis of the serum proteome in early CTCL patients using isobaric tags for relative and absolute quantification (iTRAQ) technology also indicated a strong link between lipid metabolism and CTCL development.[12] Despite extensive research into the molecular mechanisms involving FABP5 in cancer, studies focusing on its relevance in CTCL remain limited.

In this study, we examined the effects of FABP5 and the novel FABP5 inhibitor BMS-309403 on the biological behavior of CTCL and preliminarily investigated the potential of FABP5 as a therapeutic target for CTCL.

Methods

Patients and tissue specimens
This study was conducted in accordance with the Declaration of Helsinki (2013, 8th revision). The protocol (2023KA063) was reviewed and approved by the Medical Ethics Committee of Hangzhou Third People's Hospital.

Informed consent was obtained from all participants. A total of 8 samples were collected from two patients with advanced MF and one matched healthy control (HC). One patient was diagnosed with MF1 and the other had MF2 (large cell transformation). The samples included four skin lesions at different stages of MF, two adjacent tissues, and a peripheral blood mononuclear cell (PBMC) sample from the MF1 patient [Supplementary Table S1]. All tissue samples were assessed and dissected by two experienced pathologists.

Single-cell RNA sequencing bioinformatic and statistical analysis
The samples were prepared as single-cell suspensions, and sequencing and data analysis were performed by Shanghai Ouyi Biomedical Technology Co. The official 10x Genomics software, CellRanger, was used to generate data quality statistics and compare it to the reference genome in order to obtain high-quality information.

The cells were then categorized into subpopulations. Copy number variation (CNV) values for each chromosomal region were assessed using the InferCNV package (v1.0.4) based on gene expression in single-cell transcriptome data. T-lymphocytes were identified as cancer cells, and the remaining cells were classified as normal cells. Genes were sorted by their chromosomal locations, and the average gene expression was calculated using a sliding window size of 101 genes. The expression data from normal cells was used as a control to remove noise and generate the final CNV result file. Raw sequence data from the 10X Chromium experiments were analyzed using the Cell Ranger package (v3.1).

Cell culture
The human cutaneous T-cell lymphoma cell line, Hut-78 (Fuheng Biology, Shanghai, China, CL0364), was cultured in RPMI-1640 medium (Gibco, USA) supplemented with 10% fetal bovine serum (FBS, Gibco, USA) and 1% penicillin (Hyclone, USA). The cells were maintained in standard culture conditions (37°C, 5% CO_2).

CTCL cells were treated with BMS-309403 (MedChemExpress (Monmouth Junction, NJ, USA) at concentrations of 25, 50, 75, 100, 125, and 150 µM for 24, 48, and 72 hours. The antibodies used in this study are listed in Supplementary Table S2.

Cell transfection and plasmid construction
Cells were transfected with lentivirus-packaged shFABP5 and FABP5 plasmids (Yunzhou Biosciences Co., Ltd., Guangzhou, China) using the HighGene transfection reagent (Abclonal, USA). Stably transfected cells were selected using puromycin (2.5 µg/mL, Thermo Fisher Scientific, Waltham, MA) for further analysis, and transfection efficiency was assessed by RT-qPCR. An empty lentiviral vector was used for transfection in the short hairpin RNA-negative control (sh-NC) group [Supplementary Table S3].

Quantitative real- time PCR
Total RNA was extracted from cells using the TRIzol reagent (Invitrogen, USA) according to the manufacturer's protocol. A specific cDNA synthesis kit (Tiangen, Beijing, China) was used for cDNA synthesis, with reverse transcription performed at 42°C for 15 minutes followed by 95°C for 3

minutes. Quantitative real-time PCR was carried out using the SYBR Green PCR Master Mix (Lifeint, Xiamen, China), with Glyceraldehyde 3-phosphate dehydrogenase (GAPDH) serving as the internal control.

Cell counting Kit-8 and transwell migration assay

The proliferation of CTCL cells was assessed using the CCK-8 assay. Cells were plated at a density of 2000 cells/well in 96-well plates and CCK-8 solution (Beyotime Biotechnology, Shanghai, China) was then carefully added to each well (10 μL/well). The cells were incubated for 2 hours at 37°C, and the optical density (OD) was measured at 450 nm using a microplate reader (Wuxi Hiwell Diatek, DR-3518G).

In the transwell migration assay, the upper chambers were pre-coated with Matrigel (Corning, NY, USA) for 4 hours and cells (1 × 10⁶) were seeded in 200 μL of serum-free medium. Complete medium containing 10% FBS was added to the lower chamber. After incubation at 37°C for 24 hours, the cells were fixed with 4% paraformaldehyde for 30 minutes and stained with 0.1% crystal violet (Beyotime Biotechnology, Shanghai, China) for 20 minutes. The stained cells were then counted under a microscope.

Western blotting and enzyme-linked immunosorbent assay

Proteins were extracted using Radio immunoprecipitation assay (RIPA) lysis buffer (Beyotime Biotechnology, Shanghai, China), and total protein concentrations were quantified using a Bicinchoninic acid (BCA) protein assay kit (Beyotime Biotechnology, Shanghai, China). Equal amounts of protein were separated by 10% Sodium Dodecyl Sulfate-Polyacrylamide Gel Electrophoresis (SDS-PAGE) gels and electrotransferred onto polyvinylidene fluoride (PVDF) membranes. The membranes were blocked with 5% defatted milk at room temperature for 1 hour, followed by overnight incubation with primary antibodies at 4°C. After four washes with TBST (Tris-buffered saline containing 0.1% Tween®20 detergent), the proteins were incubated with secondary antibodies, and the immunoreactive bands were visualised using enhanced chemiluminescence (ECL). Cell supernatants were collected, and TC and TG levels were determined using enzyme-linked immunosorbent assay (ELISA) kits.

Quantification of FAs, TC, TG and FA uptake assay

The concentrations of FA, TC, and TG in CTCL cells were measured using the FA Assay Kit (mlsw0490), Free Cholesterol Assay Kit (mlsw0502), and Glycerol Assay Kit (mlsw0501), following the manufacturer's protocols (Mlbio, Shanghai, China). FA uptake in CTCL cells was evaluated using the FA Uptake Assay Kit (MAK156, Sigma-Aldrich).

Flow cytometry analysis

An Annexin V conjugated with Fluorescein Isothiocyanate (V-FITC) detection kit (Beyotime Biotechnology Co.) was used for the apoptosis assay and cellular apoptotic rates were evaluated by flow cytometry (Beckman, USA). All samples were analyzed on a BD LSRFortessa, and the data were analyzed using CELL Quest software. Accumulating evidence has demonstrated that FABP5 participates in lipid metabolism, cell growth, immune response, and in the development and progression of various cancers.[13,14]

Statistical analyses

The R language (v3.6.3) was utilized for statistical analysis of public datasets. The data in this study were subjected to more than three independent experiments and statistically processed using SPSS software. A t-test in a completely randomized design was applied to compare data between two groups, while one-way Analysis of variance (ANOVA) was used to compare data across multiple groups.

qPCR data were analysed using the ΔΔCt method. The data were first normalized to the reference gene, and the relative expression levels of the target gene were then calculated. Differences between groups were assessed using one-way ANOVA. Statistical significance was defined as $P < 0.05$, with the following p-values indicating the levels of significance: *$p \leq 0.05$, **$p \leq 0.01$, ***$p \leq 0.001$, and ****$p \leq 0.0001$.

Results

FABP5 is upregulated in human CTCL tissues and cells

To assess the expression of FABP5 in CTCL, single-cell transcriptomic analysis was conducted on eight skin samples (two advanced MF patients and a matched healthy control) [Figure 1a]. Samples were group into 16 unsupervised clusters and visualized by Uniform Manifold Approximation and Projection (UMAP), and we performed large-scale copy number variations (CNVs) analysis to define the malignant cells [Figures 1b and 1c].

A significant increase in FABP5 expression in malignant T-cell subtypes was noted, particularly in clusters C02, C11, C13, and C16 [Figure 1d]. Pseudotime analysis revealed that FABP5 was upregulated along with the T-cell differentiation trajectory [Figures 1e and 1f]. Two other lipid metabolism-associated genes, FASN and SREBP1, also exhibited increased expression in several malignant T-cells from CTCL [Figure 1g]. These results were confirmed by the demonstration of elevated FABP5 expression in the CTCL cell line using qRT-PCR, compared to Peripheral blood mononuclear cells (PBMCs) at the mRNA level [Figure 1h].

This suggests that the upregulation of FABP5 could play a role in the malignant progression of CTCL.

FABP5 silencing suppressed proliferation, invasion and induced apoptosis of CTCL cells

To investigate the role of FABP5 in CTCL, loss-of-function experiments were conducted by generating CTCL cell lines with stable FABP5 knockdown using shRNA lentiviruses. Transfection efficiency was confirmed by qRT-PCR. As shown in Figure 2a, FABP5 mRNA levels were significantly lower in the knockdown group compared to the control groups ($p < 0.01$). FABP5 knockdown inhibited cell proliferation,
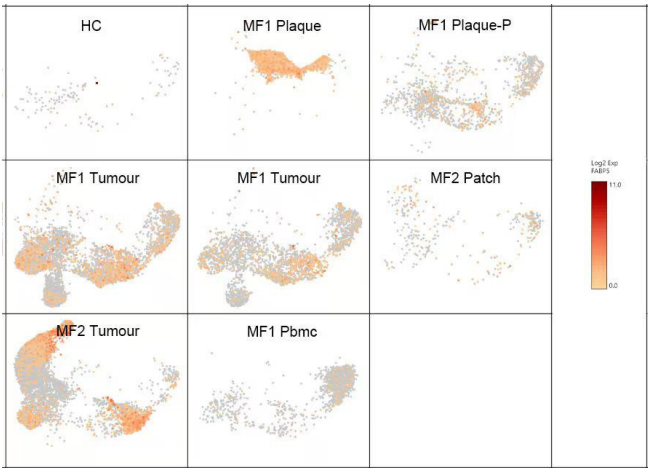
Figure 1a: The expression of *FABP5* in CTCL cells and tissues. *FABP5* expression in all T-cells of control and CTCL group samples consist of MF1 patients (plaque, plaque paraneoplastic, tumour, tumour paraneoplastic, and PBMC), MF2 patients (patch, tumour), and HC.
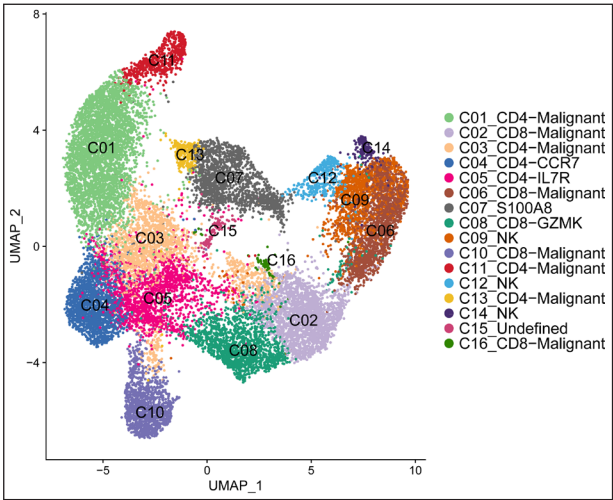

Figure 1b: The expression of *FABP5* in CTCL cells and tissues. (b-c) UMAP showed T-cells clustered individually into 16 cell subpopulations and expression of *FABP5* on UMAP.
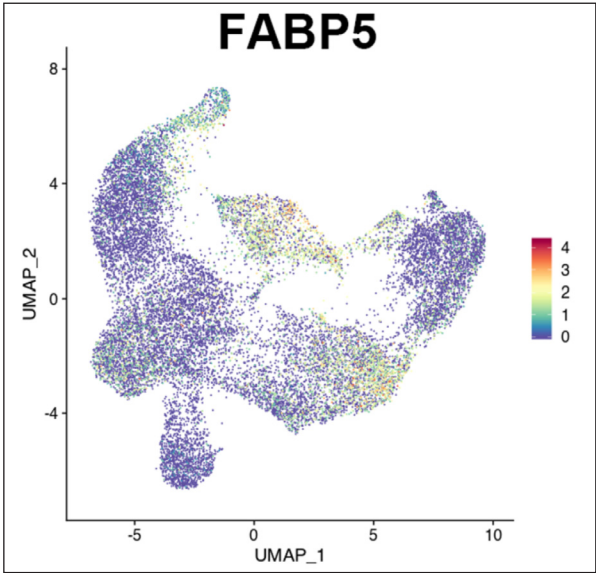

Figure 1c: UMAP visualization of FABP5 expression patterns in CTCL tissues. The colour gradient from dark to bright represents increasing FABP5 expression levels.

as measured by the Cell counting kit-8 (CCK-8) assay [p < 0.01; Figure 2b], and reduced cell migration and invasion, as assessed by the transwell assay (p < 0.01) [Figures 2c and 2d].

Flow cytometry analysis of cell cycle distribution and apoptosis levels revealed that FABP5 knockdown significantly decreased the percentage of cells in the S phase, while increasing the proportion of cells in the G0/G1 phases [Figures 2e and 2f]. Specifically, the population of cells in the G0/G1 phase was notably higher in the FABP5 shRNA-transfected group compared to the control groups, indicating that FABP5 knockdown induces cell cycle arrest at the G0/G1 phase (p < 0.01). Additionally, this group exhibited a significantly higher proportion of apoptotic cells, suggesting that silencing FABP5 promotes apoptosis in CTCL cells (p < 0.01) [Figures 2g and 2h].

Depletion of FABP5 blocks CTCL cells EMT and regulates FA metabolism

The impact of FABP5 on the EMT process was evaluated using qRT-PCR and Western blot analysis to investigate
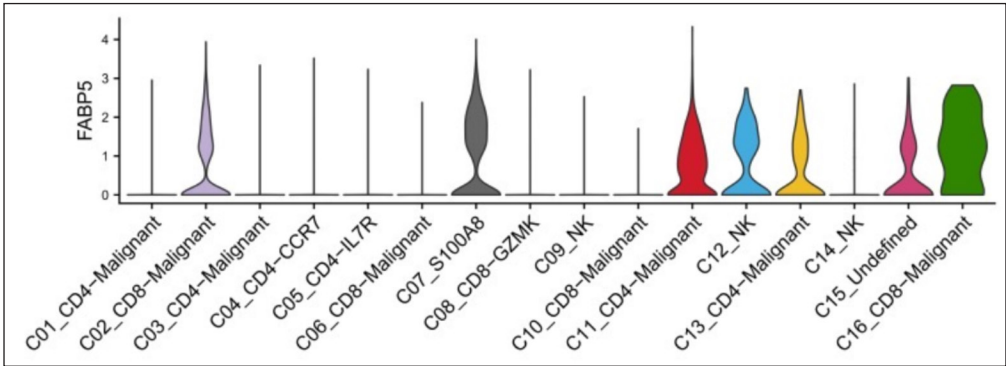

Figure 1d: The expression of *FABP5* in CTCL cells and tissues. Increased expression of the tumour-associated gene **FABP5** in malignant T-cell subsets. *FABP5* expression was significantly elevated in malignant T-cell subsets (C02, C11, C13, C16).
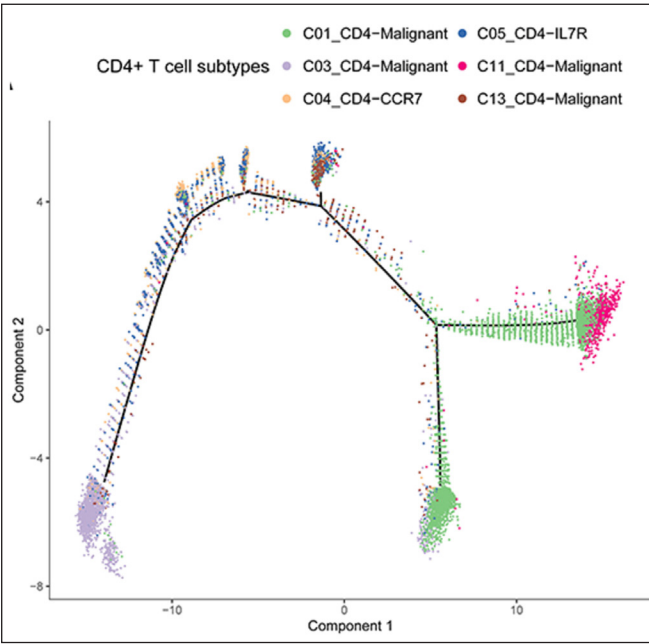
Figure 1e: The expression of *FABP5* in CTCL cells and tissues. Plot of the proposed time trajectory of CD4+ T-cell differentiation, each point represents a cell.
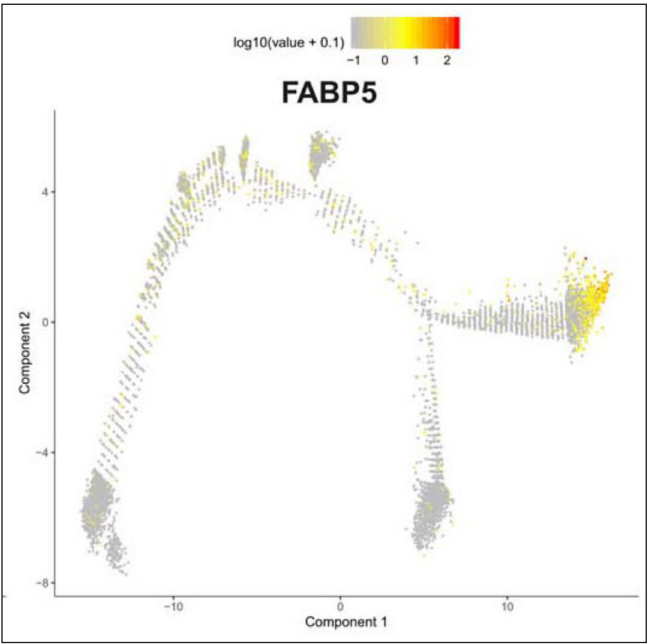

Figure 1f: The expression of *FABP5* in CTCL cells and tissues. Mapping of *FABP5* expression levels on the proposed temporal trajectory, with colours ranging from grey to yellow, representing low to high gene expression.
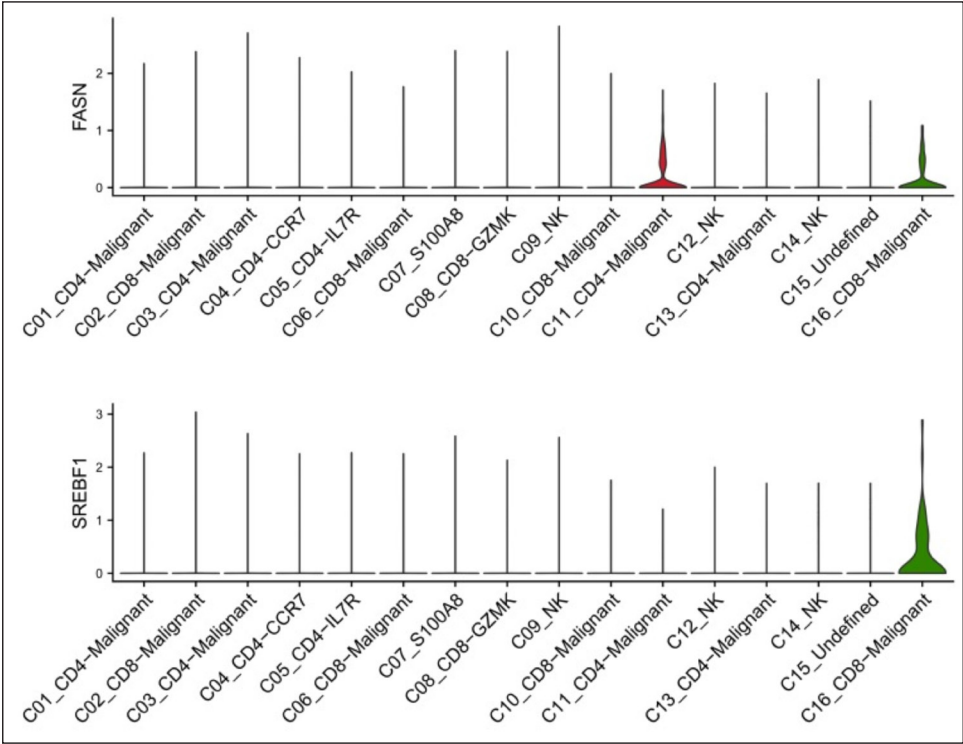

Figure 1g: The expression of *FABP5* in CTCL cells and tissues. Expression of *SREBP1* and *FASN* in various subpopulations of T-cells. *FASN* and *SREBP1* expression was significantly elevated in C11, C16, and C16 subsets.

its effect on CTCL cell proliferation. FABP5 knockdown reduced N-cadherin and VEGF expression, while increasing E-cadherin expression at both the mRNA and protein levels ($p < 0.01$) [Figures 3a-3g].

The effects of FABP5 knockdown on FA synthesis in CTCL were assessed by measuring intracellular levels of free FAs, TC, and TG to evaluate lipolytic activity. Inhibition of FABP5 resulted in a significant reduction of free FAs ($p < 0.01$), TGs ($p = 0.002$), and TCs ($p < 0.01$) [Figure 3h].
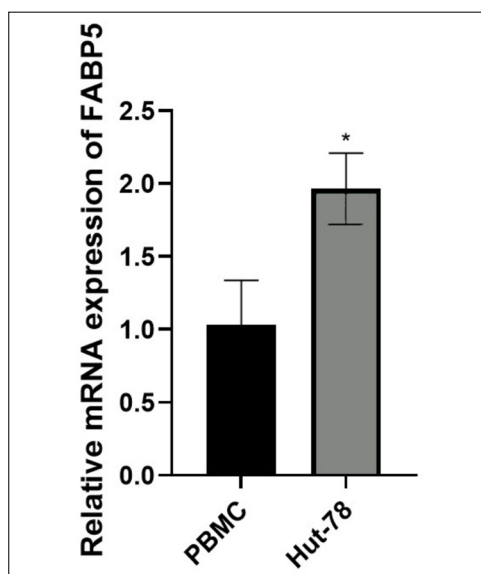
Figure 1h: The expression of *FABP5* in Hut-78 (a CTCL cell line) and tissues. *FABP5* is highly expressed in the CTCL cell line. *p ≤ 0.05.

FABP5 inhibitor BMS-309403 inhibits cell activity, fatty acid synthesis and uptake in CTCL cells

The effect of pharmacological inhibition of FABP5 on cell viability and apoptosis in CTCL cells was evaluated by treating the cells with BMS-309403 at various concentrations using the CCK-8 assay and apoptosis analysis. BMS-309403 reduced cell viability in a dose-dependent manner, with a maximum inhibition of approximately 62% at 125 µM (p < 0.0001) [Figure 4a], and increased apoptosis, particularly at higher concentrations and longer treatment durations (p < 0.001) [Figure 4b].

BMS-309403 treatment also lowered TC (p < 0.01) and TG (p < 0.0001) levels, while the FABP5 group showed an increase in both TC (p < 0.05) and TG (p < 0.01) levels [Figure 4c]. This suggests that FABP5 facilitates fatty acid uptake, increasing intracellular FAs and activating PPARγ, a key player in lipid metabolism. The expression of p-PPARγ, downstream of FABP5, significantly decreased compared to the control (p < 0.01) (p < 0.01) [Figure 4d]. Additionally, an FA uptake assay showed that BMS-309403 inhibited FA uptake in a dose-dependent manner, reducing uptake by 51.1% at 100 µM (p < 0.001) [Figure 4e].

Discussion

CTCL is an indolent lymphoproliferative disorder characterised by aberrant T-cell proliferation, but drug resistance and unpredictable, aggressive progression present significant challenges in its management.

Growing evidence suggests that FABP5 plays a role in lipid metabolism, cell growth, immune response, and the development and progression of various cancers, including CTCL. However, the exact biological role and molecular mechanisms by which FABP5 contributes to cancer development, particularly in CTCL, remain unclear.[13,14]

This study investigated the oncogenic role of FABP5 in CTCL in vitro using FABP5 knockdown and the FABP5 inhibitor BMS-309403 in cell lines. The results showed that FABP5 is upregulated in CTCL cells, and its silencing effectively inhibited cell proliferation, survival, and invasion. Silencing FABP5 also led to a significant reduction in FA, TG, and TC levels, highlighting its crucial role in reprogramming fatty acid metabolism in CTCL. These findings suggest that FABP5 could be a promising therapeutic target for CTCL.
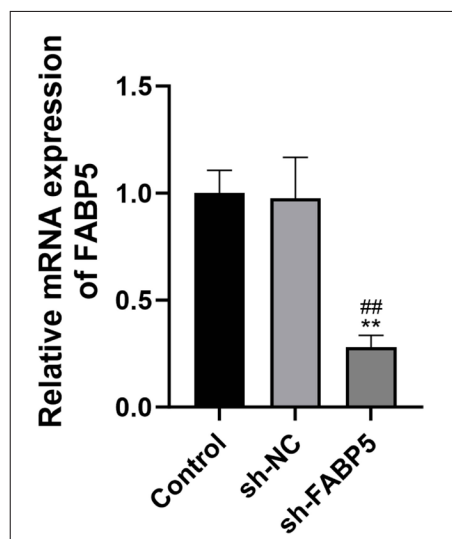

Figure 2a: Knockdown of *FABP5* suppresses cell proliferation, migration, and invasion. qRT-PCR of the mRNA levels of *FABP5* in sh-FABP5, sh-NC, and control. * *P < 0.01 and # # P < 0.01.
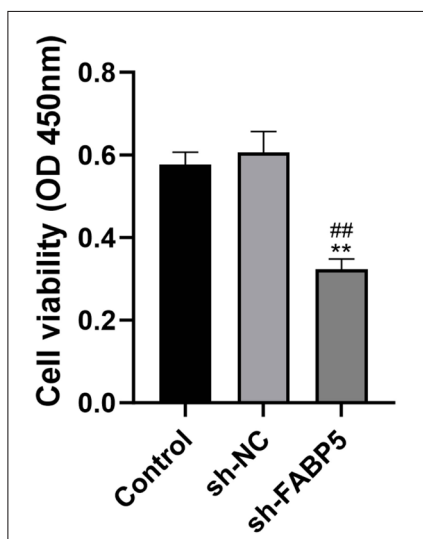
Figure 2b: Knockdown of *FABP5* suppresses cell proliferation, migration, and invasion. CCK-8 assays showing that knockdown of *FABP5* repressed the cell proliferation. * *P < 0.01 and # # P < 0.01.
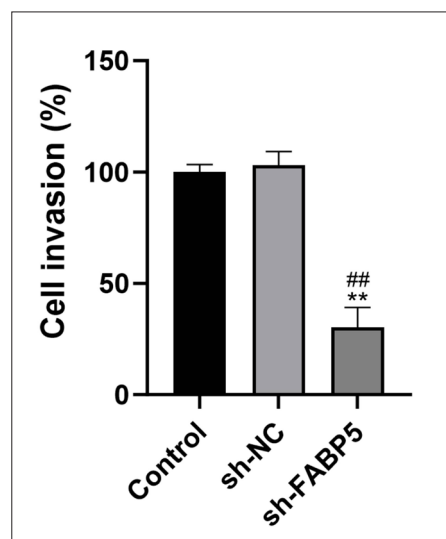
Figure 2c: Transwell assay results showing the effects of *FABP5* on the invasive capacity of CTCL cells. The invasion ability of CTCL cells decreased when knockdown of *FABP5*. * *P < 0.01 and # # P < 0.01.
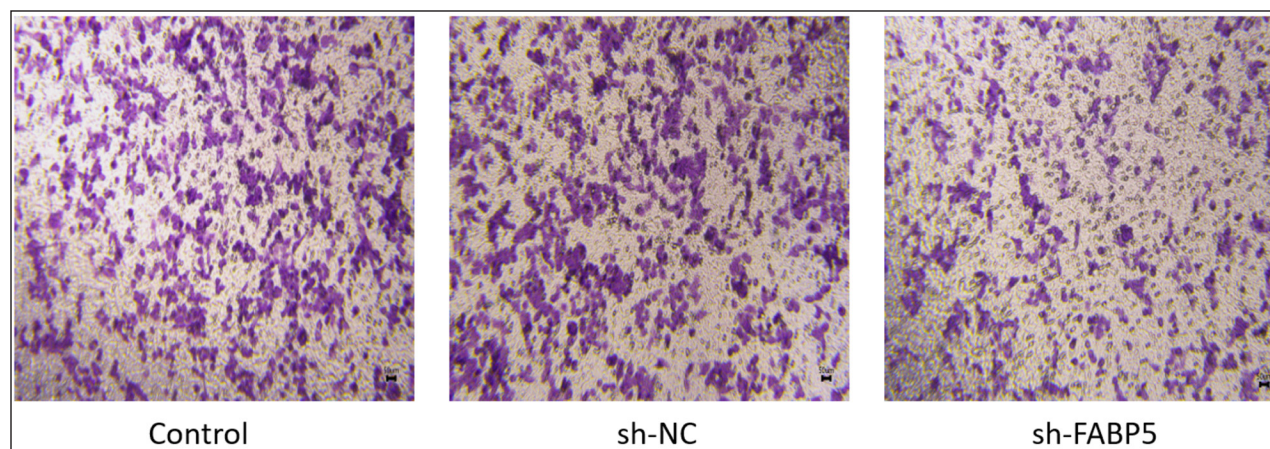
Figure 2d: Knockdown of *FABP5* suppresses cell proliferation, migration, and invasion. Transwell assay was conducted to investigate the effects of *FABP5* on the invasive capacity of CTCL cells, and it indicated that the invasion ability of CTCL cells decreased when the expression of *FABP5* decreased. The image was obtained using bright-field microscopy at a magnification of 100x with a scale bar of 50 μm. Cells were stained with crystal violet to visualize migrated or invaded cells.

Elevated levels of endogenous FA biosynthesis are observed in various cancer types, likely driven by their heightened proliferation rates.[15,16] FABP5 plays a crucial role in tumour lipid metabolism and contributes to oncogenesis by regulating fatty acid uptake, lipid storage, and key signalling pathways, which promote cell survival, proliferation, and angiogenesis across various cancers. In cutaneous T-cell lymphoma (CTCL), overexpression of FABP5 may alter lipid metabolism, contributing to the malignant progression of CTCL cells.

FABP5 promotes lymph node metastasis in cervical cancer by regulating fatty acid metabolism and activating the NF-kB pathway.[17] In hepatocellular carcinoma, the FA-induced FABP5/Hypoxia-inducible factor (HIF)-1α axis enhances ACSL1 expression and other genes involved in lipid droplet formation, reprogramming lipid metabolism and boosting cell proliferation.[4] In pancreatic neuroendocrine neoplasms, FABP5 functions as an oncogene, driving tumour progression by promoting lipid droplet accumulation and activating the WNT/β-catenin signalling pathway.[18] In prostate and breast cancer, FABP5 influences lipid metabolism by regulating key lipogenic enzymes like Hormone sensitive lipase (HSL), Monoacylglycerol lipase (MAGL), and the FABP5-PPARs signalling axis, accelerating tumour growth.[19]

In light of its role in promoting tumourigenesis, in vitro studies have explored the inhibition of FABP5 across different cancer types. The FABP5/7 inhibitor SBFI26 reduced the viability of PC3 prostate cancer cells by 25% at concentrations of 75 and 100 μM.[20] In brain cancer cells, the FABP3/4/5 inhibitor BMS309403 significantly inhibited glioblastoma cell lines, with a combination of all-trans retinoic acid (RA) further reducing cell viability by 28%.[21] Additionally, Chen *et al*. showed that resveratrol, a novel inhibitor of FABP5, inhibited migration and metastasis in cervical cancer cells in a concentration-dependent manner.[22] These studies collectively suggest that pharmacological inhibition of FABP5 reduces cell viability, inhibits invasion, and promotes apoptosis in cancer cells.

A significant finding in our study was that the inhibition of FABP5 by BMS-309403 led to the downregulation of the p-PPARγ gene, a key member of the nuclear receptor (NR) superfamily and one of the most extensively studied ligand-induced transcription factors [Figure 5]. Dysregulation of p-PPARγ signalling has been linked to tumour development and it is also involved in the FABP5-PPARγ-VEGF signalling pathway.[23] This pathway plays a crucial role in desmoplastic-resistant prostate and breast cancers, positioning FABP5 as a potential therapeutic target.[18,24-26]

Transport of excess FAs to the nucleus activates the nuclear receptor PPARγ, which regulates the expression of downstream genes to promote tumour cell proliferation, enhance invasiveness, increase angiogenesis, and reduce apoptosis. FASN produces FAs, which act as ligands for PPARγ, activating its signalling by forming heterodimers with Retinoid X receptor (RXR). These heterodimers bind to Peroxisome proliferator response elements (PPREs) in the promoter regions of target genes, regulating their transcription. Additionally, SREBP activates genes related to fatty acid synthesis, such as FASN, boosting FA production and indirectly activating PPARγ signalling. [Figure 6]. The FABP5 inhibitor likely functions by inhibiting FABP5/PPARγ signalling in CTCL cells, but further studies are needed to confirm this.

Epithelial-mesenchymal transition (EMT) is a process wherein cells lose epithelial characteristics and gain mesenchymal phenotypes, critically promoting tumor progression and metastasis.[27,28] FABP5 may facilitate reprogramming of lipid metabolism in tumour cells to meet the bioenergetic demands of EMT. In our study the deletion of FABP5 reduces EMT by suppressing EMT-related proteins in CTCL cells, ultimately inhibiting tumourigenesis and progression. Additionally, the
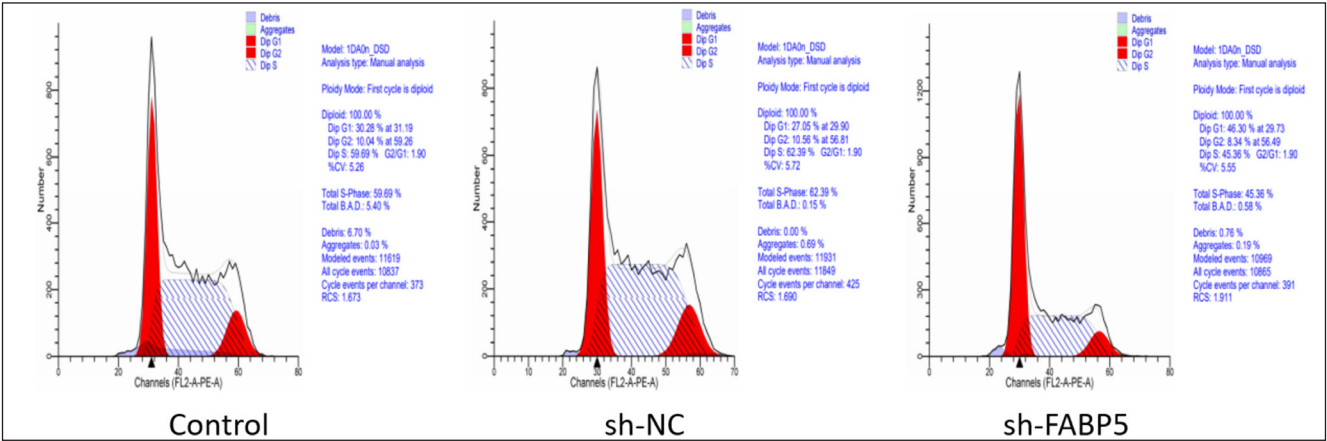
Figure 2e: Knockdown of *FABP5* suppresses cell proliferation, migration, and invasion. Flow cytometry to detect cell cycle and apoptosis levels. Statistical analysis was performed according to the data of three independent experiments. * *P < 0.01.
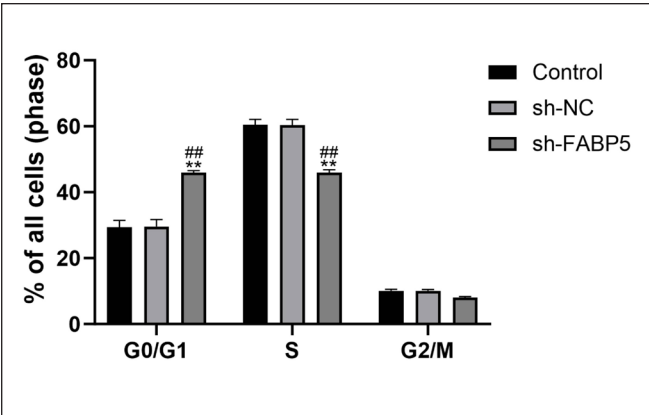

Figure 2f: Flow cytometry to assess cell cycle distribution. The percentage of cells in each phase (G0/G1, S, G2/M) is shown for Control, sh-NC, and sh-*FABP5* groups. * *P < 0.01 and # # P < 0.01.
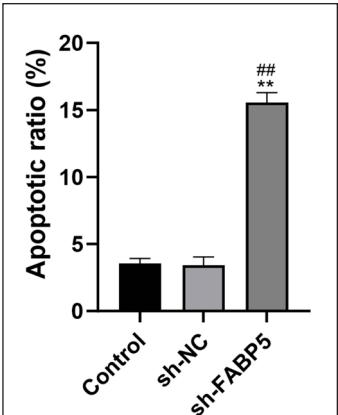
Figure 2g: Flow cytometry to measure apoptotic ratio. The percentage of apoptotic cells is shown for Control, sh-NC, and sh-*FABP5* groups. * *P < 0.01 and # # P < 0.01.
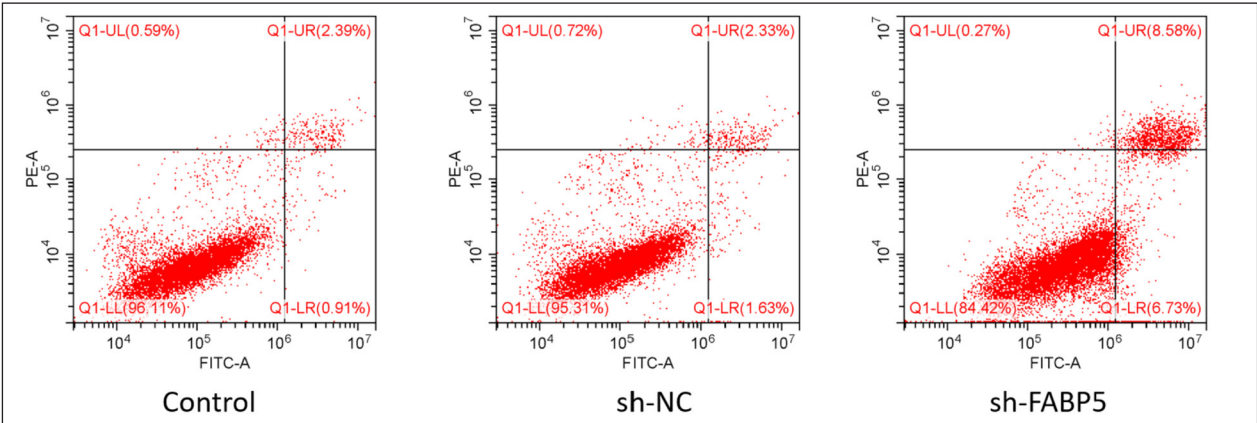
Figure 2h: Flow cytometry analysis was performed to evaluate the effects of *FABP5* on CTCL cell. The results suggest that knockdown of *FABP5* promotes cell apoptosis.
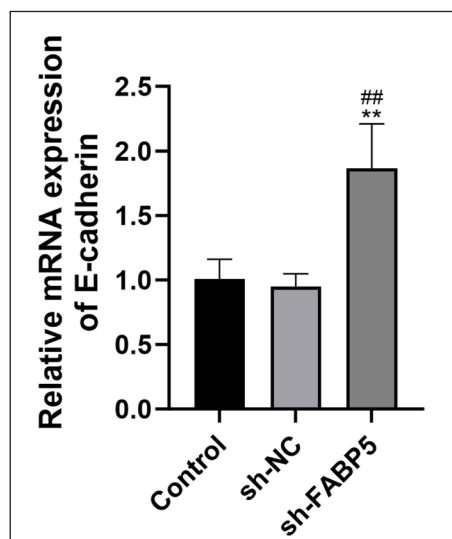
Figure 3a: Depletion of *FABP5* blocks EMT and regulates lipid metabolism in CTCL. qRT-PCR and western blot revealed E-cadherin, N-cadherin, and VEGF in the CTCL cell line. Statistical analysis was performed according to the data of three independent experiments. * *P < 0.01 and # # P < 0.01.
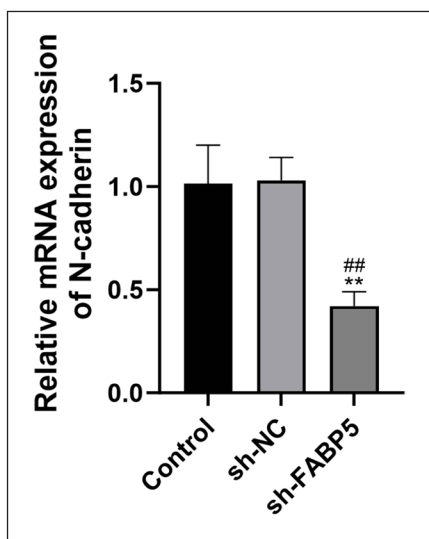
Figure 3b: qRT-PCR analysis revealed that the expression of N-cadherin in CTCL cells decreased after the knockdown of *FABP5*. The bar colours in the graph represent different experimental groups: Control is represented in black, sh-NC in light gray, and sh-*FABP5* in dark gray. * *P < 0.01 and # # P < 0.01.
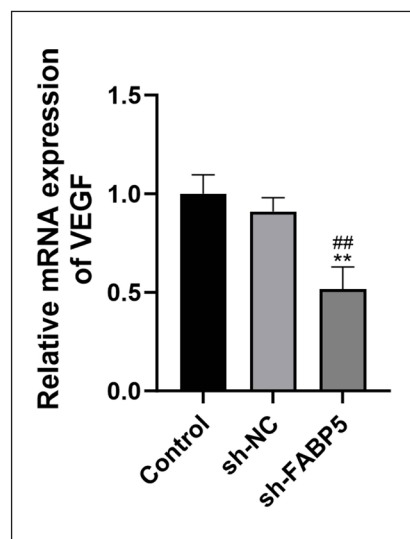
Figure 3c: qRT-PCR analysis showed a reduction in VEGF expression in CTCL cells following the knockdown of *FABP5*. The bar colours in the graph represent different experimental groups: Control is represented in black, sh-NC in light gray, and sh-*FABP5* in dark gray. * *P < 0.01 and # # P < 0.01.
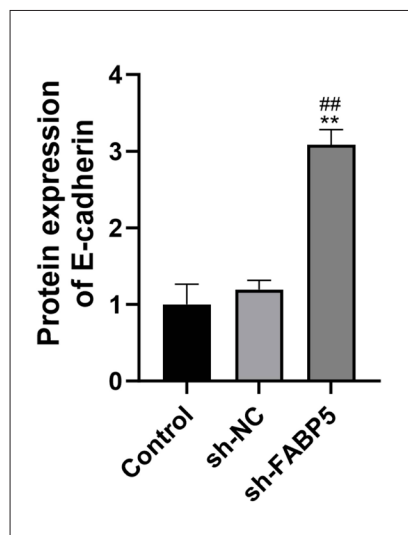
Figure 3d: Western blot analysis showed an increase in E-cadherin expression in CTCL cells following the knockdown of *FABP5*. The bar colours in the graph represent different experimental groups: Control is represented in black, sh-NC in light gray, and sh-*FABP5* in dark gray. * *P < 0.01 and # # P < 0.01.
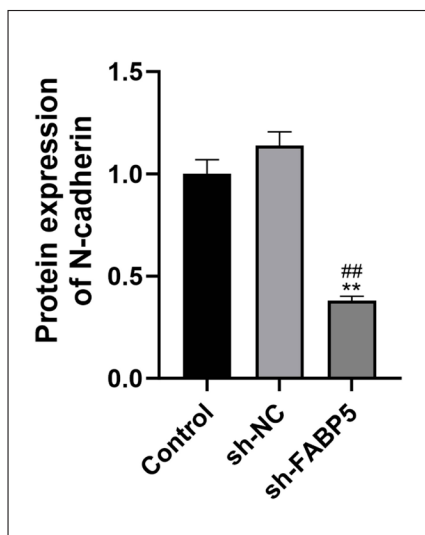
Figure 3e: Western blot analysis showed a reduction in N-cadherin expression in CTCL cells following the knockdown of *FABP5*. The bar colours in the graph represent different experimental groups: Control is represented in black, sh-NC in light gray, and sh-*FABP5* in dark gray. * *P < 0.01 and # # P < 0.01.
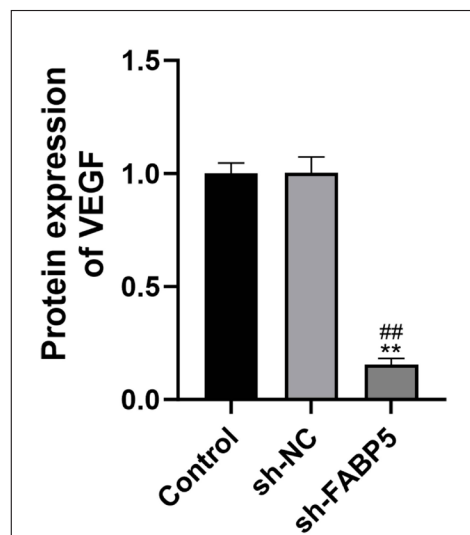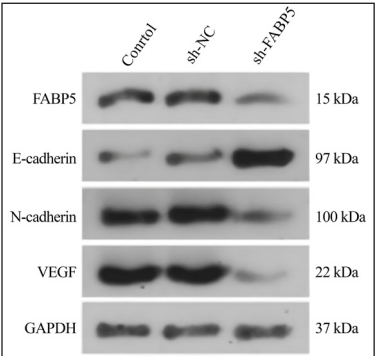
Figure 3f: Western blot analysis indicated that VEGF expression in CTCL cells was reduced after the knockdown of *FABP5*. The bar colours in the graph represent different experimental groups: Control is represented in black, sh-NC in light gray, and sh-*FABP5* in dark gray. * *P < 0.01 and # # P < 0.01.

Figure 3g: Western blot analysis of E-cadherin, N-cadherin, and VEGF expression in Control, sh-NC, and sh-*FABP5* groups. The results demonstrate changes in the expression levels of these markers following the knockdown of *FABP5* in CTCL cells.
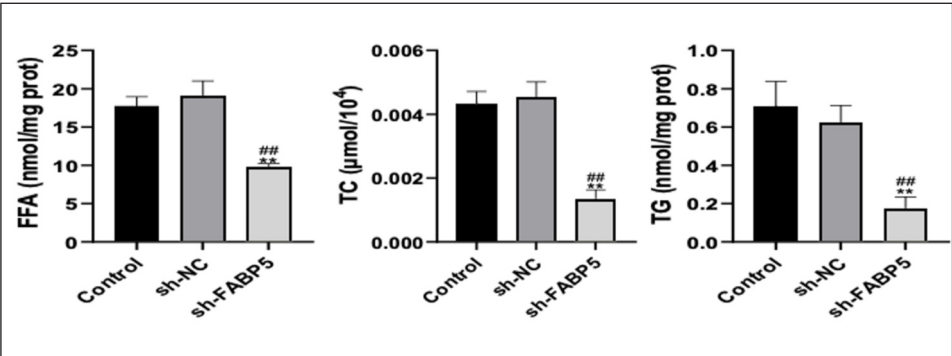
Figure 3h: In the figure, the bar colours represent different experimental groups: Control is represented in black, sh-NC in light gray, and sh-*FABP5* in dark gray. * *P < 0.01 and ## P < 0.01.
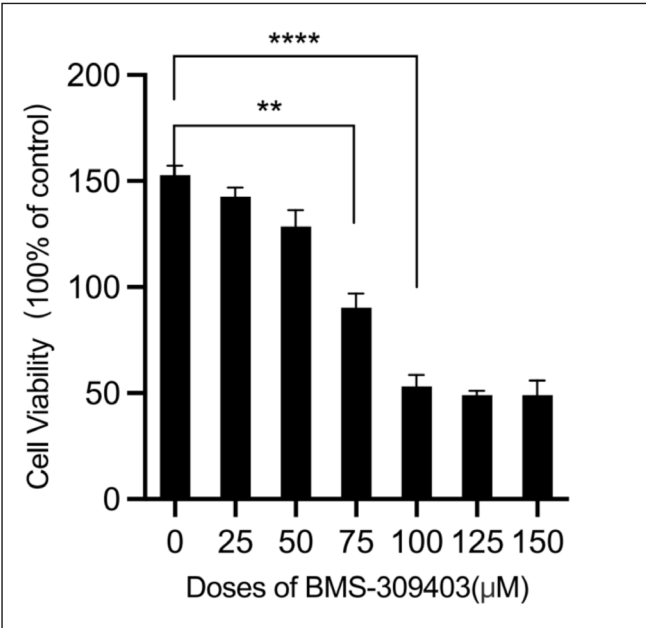

Figure 4a: *FABP5* silencing inhibited CTCL progression through regulating lipid metabolism. CCK-8 assay was used to assess the viability of CTCL cells treated with BMS-309403 at different concentrations. *P < 0.01 and # # P < 0.01.
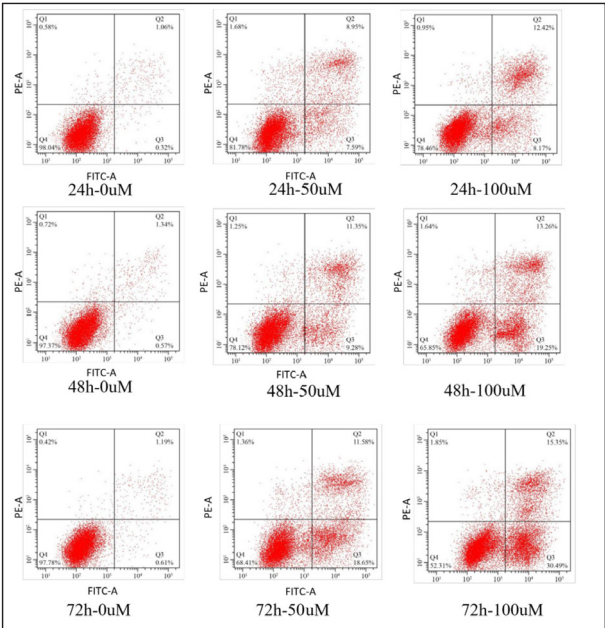
Figure 4b: *FABP5* silencing inhibited CTCL progression through regulating lipid metabolism. Flow cytometry analysis was detected to evaluate the apoptosis of BMS-309403 treated CTCL cells. Statistical analysis was performed according to the data of three independent experiments.
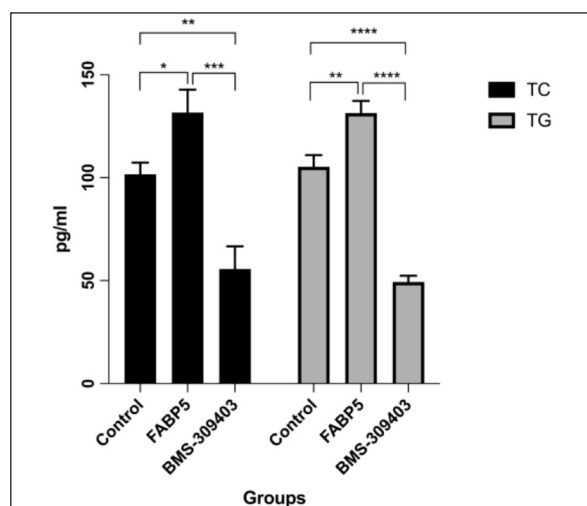
Figure 4c: *FABP5* silencing inhibited CTCL progression through regulating lipid metabolism. Effect of *FABP5* and BMS-309403 on the synthesis of TC and TG in CTCL cells. $*P < 0.01$ and $\# \# P < 0.01$.
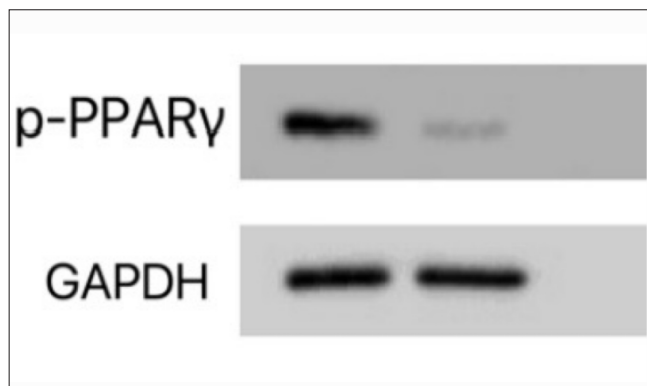

Figure 4d: *FABP5* silencing inhibited CTCL progression through regulating lipid metabolism. Western blot was applied to measure SREPB1 and p-PPARγ expression.
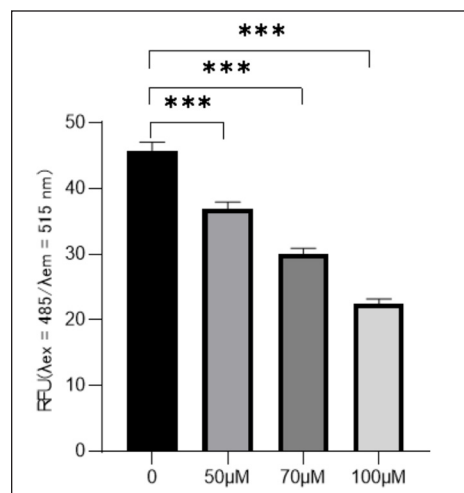

Figure 4e: In the figure, the bar colours represent different experimental groups: the bar for 0 μM can be coloured black, 50 μM gray, 70 μM dark gray, and 100 μM light gray $* * *P < 0.001$
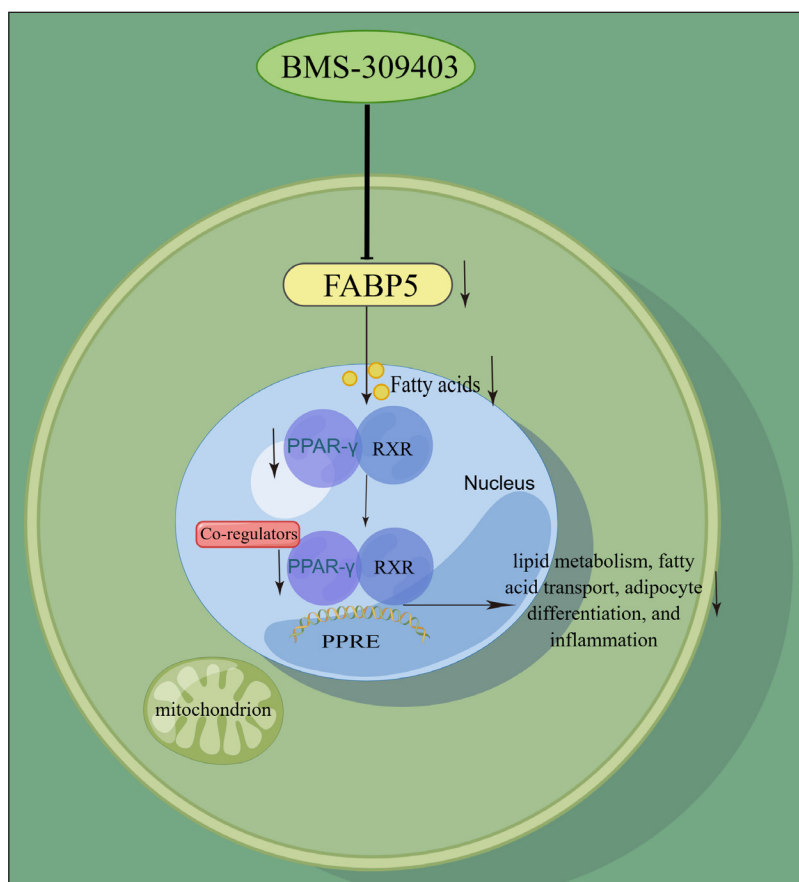

Figure 5: The change of the *FABP5*/PPARγ signalling pathway and associated molecules after the application of the inhibitor BMP309403.
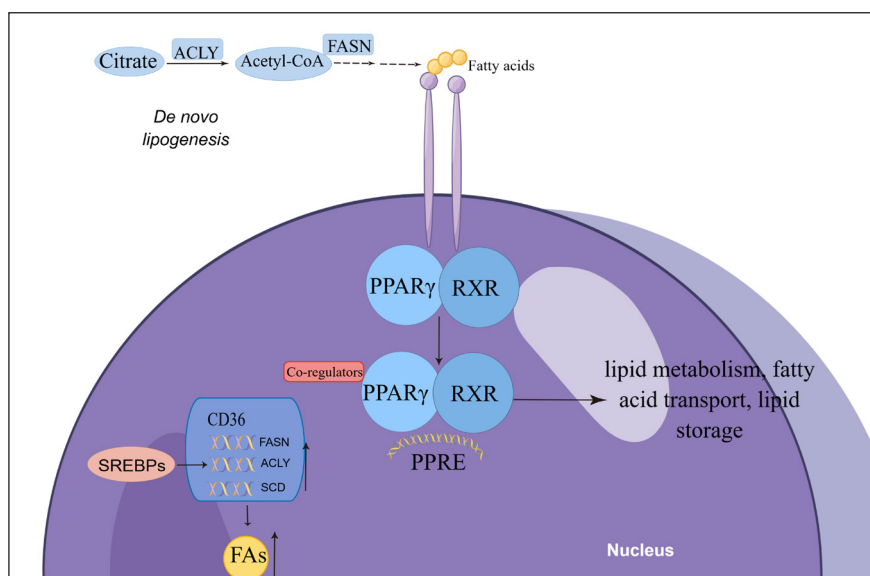
Figure 6: The mechanistic links between FASN, SREBP, and PPARγ signalling.

connection between FABP5 and VEGF may help explain the observed increase in tumour angiogenesis, considering the critical role of VEGF proteins in angiogenesis.

Limitations

In our study, we did not perform in vivo experiments to further validate our findings. Additionally, the precise site of action of FABP5 in CTCL remains unclear. Further investigations are required to elucidate the underlying mechanisms.

Conclusion

In this study, we examined FABP5 expression in CTCL cells and its role in cell proliferation, invasion, and lipid metabolism. Our findings identify FABP5 as a key regulator of CTCL cell proliferation and fatty acid metabolism, highlighting its role in limiting tumour growth and spread.

Thus, the FABP5/PPARγ axis emerges as a promising therapeutic target, with BMS-309403 showing potential as a novel agent for CTCL treatment. Targeting lipid metabolism, with FABP5 as a central focus, could offer an effective approach for cancer therapy.

References

1. Willemze R, Cerroni L, Kempf W, Berti E, Facchetti F, Swerdlow SH, *et al*. The 2018 update of the WHO-EORTC classification for primary cutaneous lymphomas. Blood 2019;133:1703-14.
2. Xia L, Oyang L, Lin J, Tan S, Han Y, Wu N, *et al*. The cancer metabolic reprogramming and immune response. Mol Cancer 2021;20:28.
3. Cheng C, Geng F, Cheng X, Guo D. Lipid metabolism reprogramming and its potential targets in cancer. Cancer Commun (Lond) 2018;38:27.
4. Seo J, Jeong DW, Park JW, Lee KW, Fukuda J, Chun YS. Fatty-acid-induced FABP5/HIF-1 reprograms lipid metabolism and enhances the proliferation of liver cancer cells. Commun Biol 2020;3:638.
5. Mukherjee A, Bilecz AJ, Lengyel E. The adipocyte microenvironment and cancer. Cancer Metastasis Rev 2022;41:575-87.
6. Smathers RL, Petersen DR. The human fatty acid-binding protein family: Evolutionary divergences and functions. Hum Genomics 2011;5:170-91.
7. Lu F, Ye M, Hu C, Chen J, Yan L, Gu D, *et al*. FABP5 regulates lipid metabolism to facilitate pancreatic neuroendocrine neoplasms progression via FASN mediated wnt/β-catenin pathway. Cancer Sci 2023;114:3553-67.
8. George Warren W, Osborn M, Yates A, Wright K, O'Sullivan SE. The emerging role of fatty acid binding protein 5 (FABP5) in cancers. Drug Discov Today 2023;28:103628.
9. Takahashi-Shishido N, Sugaya M, Morimura S, Suga H, Oka T, Kamijo H, *et al*. Mycosis fungoides and Sezary syndrome tumour cells express epidermal fatty acid-binding protein, whose expression decreases with loss of epidermotropism. J Dermatol 2021;48:685-9.
10. Liu J, Zeng Y, Zhou Y, Ma D, Wang B. Proteomic expression analysis of mycosis fungoides (MF) skin tissues: Overexpressions of SOD2, S100A8 and FABP5 in MF. J Dermatol Sci 2010;60:42-4.
11. Chi C, Harth L, Galera MR, Torrealba MP, Vadivel CK, Geisler C, *et al*. Concomitant inhibition of FASN and SREBP provides a promising therapy for CTCL. Cancers (Basel) 2022;14:4491.
12. Zhu M, Li Y, Ding C, Wang J, Ma Y, Li Z, *et al*. Proteomic profiling change and its implies in the early mycosis fungoides (MF) using isobaric tags for relative and absolute quantification (iTRAQ). Biomed Res Int 2020;2020:9237381.
13. Xu B, Chen L, Zhan Y, Marquez KNS, Zhuo L, Qi S, *et al*. The biological functions and regulatory mechanisms of fatty acid binding protein 5 in various diseases. Front Cell Dev Biol 2022;10:857919.
14. Farrell M, Fairfield H, Karam M, D'Amico A, Murphy CS, *et al*. Targeting the fatty acid binding proteins disrupts multiple myeloma cell cycle progression and MYC signalling. Elife 2023;12:e81184.
15. Mashima T, Seimiya H, Tsuruo T. De novo fatty-acid synthesis and related pathways as molecular targets for cancer therapy. Br J Cancer 2009;100:1369-72.
16. Röhrig F, Schulze A. The multifaceted roles of fatty acid synthesis in cancer. Nat Rev Cancer 2016;16:732-49.

17. Zhang C, Liao Y, Liu P, Du Q, Liang Y, Ooi S, *et al*. FABP5 promotes lymph node metastasis in cervical cancer by reprogramming fatty acid metabolism. Theranostics 2020;10:6561-80.

18. Lu F, Ye M, Hu C, Chen J, Yan L, Gu D, *et al*. FABP5 regulates lipid metabolism to facilitate pancreatic neuroendocrine neoplasms progression via FASN mediated wnt/β-catenin pathway. Cancer Sci 2023;114:3553-67.

19. Senga S, Kobayashi N, Kawaguchi K, Ando A, Fujii H. Fatty acid-binding protein 5 (FABP5) promotes lipolysis of lipid droplets, de novo fatty acid (FA) synthesis and activation of nuclear factor-kappa B (NF-κB) signalling in cancer cells. Biochim Biophys Acta Mol Cell Biol Lipids 2018;1863:1057-6.

20. Al-Jameel W, Gou X, Forootan SS, Al Fayi MS, Rudland PS, Forootan FS, *et al*. Inhibitor SBFI26 suppresses the malignant progression of castration-resistant PC3-M cells by competitively binding to oncogenic FABP5. Oncotarget 2017;8:31041-56.

21. Xia S, Wu M, Li H, Wang J, Chen N, Chen Y, *et al*. Oncotarget 2015;6:5889-902.

22. Chen X, Tian J, Zhao C, Wu Y, Li J, Ji Z, *et al*. Resveratrol, a novel inhibitor of fatty acid binding protein 5, inhibits cervical cancer metastasis by suppressing fatty acid transport into nucleus and downstream pathways. Br J Pharmacol 2024;181:1614-3.

23. Hernandez-Quiles M, Broekema MF, Kalkhoven E. PPARgamma in metabolism, immunity, and cancer: Unified and diverse mechanisms of action. Front Endocrinol (Lausanne) 2021;12:624112.

24. Al-Jameel W, Gou X, Jin X, Zhang J, Wei Q, Ai J, *et al*. Inactivated FABP5 suppresses malignant progression of prostate cancer cells by inhibiting the activation of nuclear fatty acid receptor PPARgamma. Genes Cancer 2019;10:80-96.

25. Forootan FS, Forootan SS, Gou X, Yang J, Liu B, Chen D, *et al*. Fatty acid activated PPARγ promotes tumourigenicity of prostate cancer cells by up regulating VEGF via PPAR responsive elements of the promoter. Oncotarget 2016;7:9322-39.

26. Chen NN, Ma XD, Miao Z, Zhang XM, Han BY, Almaamari AA, *et al*. Doxorubicin resistance in breast cancer is mediated via the activation of FABP5/PPARγ and caMKII signalling pathway. Front Pharmacol 2023;14:1150861.

27. Lamouille S, Xu J, Derynck R. Molecular mechanisms of epithelial-mesenchymal transition. Nat Rev Mol Cell Biol 2014;15:178-96.

28. Dongre A, Weinberg RA. New insights into the mechanisms of epithelial-mesenchymal transition and implications for cancer. Nat Rev Mol Cell Biol 2019;20:69-84.